Solid-State Photodimerization Kinetics of α-*trans*-Cinnamic Acid to α-Truxillic Acid Studied via Solid-State NMR

Marko Bertmer,† Ryan C. Nieuwendaal, Alexander B. Barnes, and Sophia E. Hayes*

Department of Chemistry and Center for Materials Innovation, Washington University, St. Louis, Missouri 63130

Received: December 20, 2005; In Final Form: February 2, 2006

The present work focuses on the topochemical photoconversion process in which α-*trans*-cinnamic acid becomes α-truxillic acid. This solid-state [2 + 2] cycloaddition reaction has previously been studied with X-ray diffraction, atomic force microscopy, and vibrational spectroscopy. However structural and kinetic details about the reaction are still debated. We present results from ^{13}C cross-polarization magic angle spinning solid-state NMR experiments that suggest that the Johnson, Mehl, Avrami, and Kolmogorov model of phase transformation kinetics can be applied to this system. The model elucidates parameters of the reaction, such as the nucleation rate, diffusion rate, and dimensionality of the reaction. From our data, it is concluded that this reaction follows one-dimensional growth with a decreasing nucleation rate.

Introduction

The study of chemical systems that undergo a structural change upon absorption of light are of interest for studying solid-state synthesis[1] and topochemistry.[2] Solid-state reactions can be attractive because, in general, the limited mobility of the reactants in the crystal lattice allows for stereochemical control of the products. For [2 + 2] photodimerization reactions, the topochemical principle predicts that a reaction occurs if the reacting double bonds are parallel to each other and their distance in the crystal lattice is less than 4.2 Å.[2]

In addition, these particular chemical systems may have potential applications in optical memory storage systems,[3,4] such as those used in holographic recording media and commercially available write-once optical disks.[4] Presently, candidate materials are those that can undergo: (1) cis−trans isomerizations, such as azobenzenes or stilbenes;[4] (2) photocyclizations, such as the fulgides,[5] diarylalkenes,[6] or spiropyrans;[7] or (3) keto−enol tautomerizations, such as salicylideneaniline.[4] A comprehensive review of these systems is given by Feringa.[3,4]

We have examined a well-known reaction, the photodimerization of α-*trans*-cinnamic acid to α-truxillic acid,[2] shown in Scheme 1, with solid-state NMR. Solid-state [2 + 2] cycloaddition reactions in α-*trans*-cinnamic acid that occur via photoirradiation routes have been studied by X-ray diffraction,[8] atomic force microscopy (AFM),[9] and vibrational spectroscopy.[10] However, these techniques all suffer from some limitations. Atomic force microscopy is sensitive primarily to surfaces, and X-ray diffraction cannot be used for characterization of amorphous solids. Furthermore, one complication of X-ray diffraction studies on molecular organic crystals was revealed in a recent study in which a similar material (4-chlorocinnamoyl-*O*,*O*′-dimethyldopamine) underwent a [2 + 2] cycloaddition as a result of the X-ray irradiation being used for characterization.[11]

The advantage of using solid-state NMR is that it is an element-selective, noninvasive spectroscopic technique that is capable of characterizing the structural differences between molecular species present in a sample including products, reactants, and possible side products. ^{13}C solid-state NMR has already been proven as a means of characterizing different polymorphs in organic crystals, particularly the photodimerization products of formyl-substituted cinnamic acid,[12] and it has been utilized for characterization of other photoreaction processes.[13,14]

SCHEME 1: Photodimerization of α-*trans*-Cinnamic Acid to α-Truxillic Acid

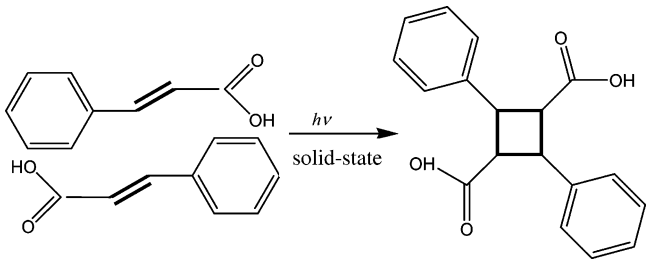

Experimental Section

trans-Cinnamic acid (Aldrich, 99%) was recrystallized from diethyl ether (Aldrich, 98%) to give the α-crystal polymorph.[15] Crystals of 100−500 μm were sieved, and approximately 60 mg was evenly distributed in a thin layer of microcrystalline powder in the focus of the lamp for the irradiation experiments. The powder sample was exposed to a 150 W xenon arc lamp (Thermo Oriel) that is equipped with a dichroic mirror to transmit wavelengths between 280 and 400 nm. Since the longer (infrared) wavelengths were blocked from the sample, the sample temperature could be maintained at room temperature (21 °C) ± 2 °C. Samples were irradiated for consecutive periods of 10−30 min of broadband light, with agitation of the powders between each consecutive period. The irradiance was measured with a Scientech power meter to be 3−4 mW/cm^2.

Solid-state NMR spectra were obtained using a 4 mm triple-resonance magic angle spinning (MAS) probe from Varian, and data were recorded using a Tecmag Apollo spectrometer.

* Author to whom correspondence should be addressed. Phone: +1 (314) 935-4624. Fax: +1 (314) 935-4481. E-mail: hayes@wustl.edu.

† Present address: Macromolecular Chemistry, RWTH Aachen University, Sammelbau Chemie, Worringer Weg 1, D-52056 Aachen, Germany.

10.1021/jp057417h CCC: $33.50
Published on Web 03/07/2006

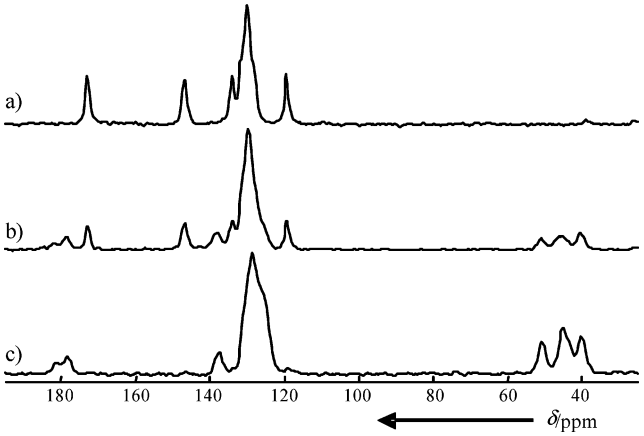

Figure 1. ^{13}C CPMAS spectra of cinnamic acid: (a) no irradiation, (b) 50% converted, and (c) 95% converted.

Resonance frequencies were 294.35 and 74.028 MHz for ^{1}H and ^{13}C, respectively. The ^{1}H $\pi/2$ pulse length was 2.5 μs, and the contact time was set to 2 ms. The recycle delay was 10 min, and the spinning speed was set to 4.5 kHz to minimize sample degradation, which was observed at higher spinning speeds. Spectra were referenced to tetramethylsilane (TMS) using adamantane as a secondary reference.

Relative ratios between the olefinic and the cyclobutane carbon signals were determined at different contact times and found to be nearly constant at contact times longer than 200 μs. This arises from the fact that they are both singly protonated carbons and that both have limited mobility. The C═C double bond cannot rotate, and the cyclobutane ring has restricted motion. Therefore, it is fairly valid to utilize the intensities from ^{13}C cross-polarization magic angle spinning (CPMAS) spectra as a quantitative measure. Furthermore, since the spectra were obtained under identical conditions (CPMAS parameters, number of scans, same amount of sample), the changes in signal intensity can directly be compared. Relative signal intensities of olefinic and cyclobutane carbons were obtained by devonvolution of the CPMAS spectra. The curve of the fraction converted versus irradiation time was repeated multiple times yielding Avrami factors of 1.6−1.7.

The UV−vis absorption spectrum, Figure 4, (190−400 nm) was taken on a Cary UV−vis spectrometer with 0.1 nm resolution. Due to solubility differences, cinnamic acid was dissolved in ethanol, and truxillic acid in petroleum ether for these measurements; however, both were at identical concentrations of 50 μM.

Results and Discussion

Figure 1 shows a series of ^{13}C CPMAS NMR[16] spectra for α-*trans*-cinnamic acid and the [2 + 2] photodimerization product recorded after different total irradiation times. Figure 1a is the parent, α-*trans*-cinnamic acid, prior to irradiation. Figure 1c indicates almost complete conversion to α-truxillic acid, and Figure 1b contains an equal mixture of both species. The complete assignments for each of the carbon sites are given in Table 1. Assignments were made based on the chemical shift ranges of individual functional groups together with spectral editing techniques, such as short contact time CPMAS and dipolar dephasing experiments.[17]

A decrease of the olefinic carbon signals is observed with a concomitant increase of the cyclobutane carbon signals. The resolution of the individual resonances and the large separation (>70 ppm) of the signals of reactant and product functional groups make the application of solid-state ^{13}C NMR ideally suited to study this class of photodimerization reactions. Additionally, the chemical shifts of the neighboring carbons, i.e., the ipso (nonprotonated aromatic) carbon and the carboxylic carbon, show a small shift between reactant and product due to differing inductive effects of the neighboring groups (vinyl vs cyclobutane). Three cyclobutane carbon signals are observed whereas only two are expected (i.e., only two types of magnetically inequivalent carbons are present—two carbons adjacent to the phenyl rings and two carbons adjacent to the carboxylic acid groups). The three signals observed here are probably due to solid-state packing effects, such as distortions of the cyclobutane ring and dihedral angle "twists" of the phenyl rings and carboxylic acid groups with respect to an idealized solution-phase structure. We believe the three signals arise as a consequence of packing in the solid state, since dissolving the reaction product in d_6-dimethylsulfoxide yields, as expected, only two cyclobutane carbon resonances. Simulations are currently underway in our laboratory to determine the solid-state conformations that yield the observed chemical shifts.

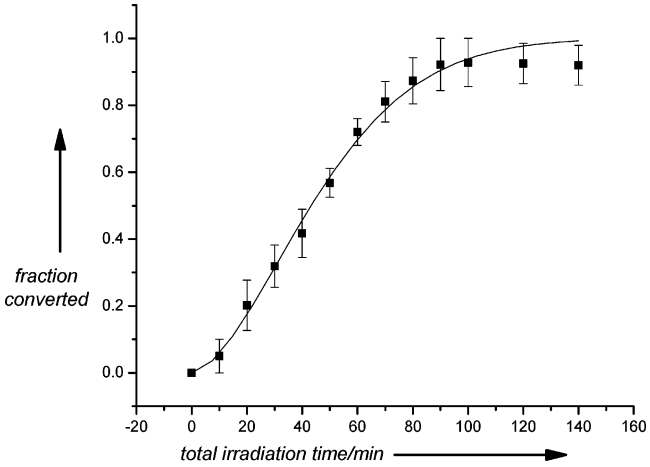

Figure 2. Rate curve of the photodimerization reaction, α-*trans*-cinnamic acid converting to α-truxillic acid. The black squares are the experimental data, and the black line corresponds to the best fit curve of the JMAK kinetics model. The n from the fit is 1.66 ± 0.10, and k is 0.019 ± 0.004 min^{-1}. Error bars are determined from the accuracy of the peak fit.

TABLE 1: Resonance Assignments for α-*trans*-Cinnamic Acid and α-Truxillic Acid

sample	δ (ppm)	assignment
α-*trans*-cinnamic acid	119	olefinic carbon (carbonyl side)
	147	olefinic carbon (phenyl side)
	127, 129, 131	protonated aromatic carbons
	134	ipso carbon
	173	carbonyl carbon
α-truxillic acid	40, 45, 51	cyclobutane carbons
	122, 128, 133	protonated phenyl carbons
	138	ipso carbon
	178, 181	carbonyl carbons

A typical curve of the fraction of cinnamic acid converted based on the relative signal intensity of cyclobutane carbons and olefinic carbons as a function of total irradiation time is shown in Figure 2. As can be seen in the figure, the plot is not simply a linear, single-exponential, or (time)$^{-1}$ curve, which would describe a zero-, first-, or second-order process, respectively.[18] Rather, we observe a sigmoidal curve. Other experiments in the literature, such as real-time vibrational spectroscopy experiments[10] with in situ photoirradiation on a single crystallite, have generated such sigmoidal-shaped curves as well. However,

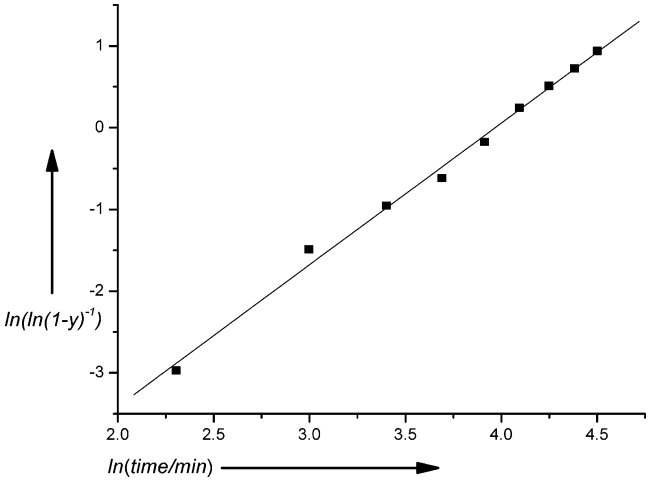

Figure 3. Avrami plot of the kinetics curve of cinnamic acid. The slope of the line, *n*, describes the growth dimensionality in the JMAK model.

to the best of our knowledge there has been no interpretation in the literature of these curves relating them to a specific kinetic mechanism.

We have fit the data to a geometrical nucleation and growth model proposed by Johnson,[19] Mehl, Avrami,[20] and Kolmogorov[21] (JMAK) that has been previously used to explain phase transformation kinetics in solids.[22] The JMAK model can be applied to a broad range of different chemical and physical transformations. The JMAK kinetics are described by

$$y = 1 - e^{(kt)^n} \quad (1)$$

where k is the rate constant of the reaction and n, the order of the reaction, describes the dimensionality of the growth of the product phase, i.e., $n = 4$ for three-dimensional growth, $n = 3$ for two-dimensional growth, and $n = 2$ for one-dimensional growth.[22] The shape of the kinetics curve gives information about how the product phase is induced and how the new phase grows, depending on the size of the order parameter, n (also known as the "Avrami exponent").

We have used this model both because the shape of the kinetics curve is suggestive of JMAK kinetics and the Avrami exponent provides us a plausible model for nucleation and growth in this system.[22] The JMAK model describes the time-dependent growth of three-dimensional objects inside an enclosed volume using several assumptions, as paraphrased by Weinberg:[23] "(1) the system is infinite in extent so that boundary terms are ignored; (2) nucleation is a uniform and independent random process; and (3) growth of particles terminates at their points of mutual contact, but continues unabated elsewhere." Simulations by Weinberg have shown that the first two assumptions need not be true for all systems. For example, it was demonstrated that the JMAK kinetics model can still be used to describe the growth process when nucleation is initiated at the surface of the material.

In a plot of ln[ln$(1 - y)^{-1}$] vs ln[time], called an "Avrami plot", the parameters of the reaction can be easily extracted.[22] A straight line with slope n is obtained; Figure 3 shows the resulting plot of the experimental data. First, the plot shows a linear dependence, which means that the process can be indicative of JMAK kinetics. Second, the slope of such a line can give insight into the growth model taking place.

If the Avrami exponent is an integer, then the nucleation rate is constant over time. However, if the nucleation rate is a decreasing function of time, then the exponent will be slightly less than the integer expected. In other words, at the onset of the reaction, nucleation centers are formed, which then proceed to grow. These nucleation centers are continuously formed throughout the reaction, but the rate at which they are formed decreases. For example, in the instance of one-dimensional growth with a decreasing nucleation rate, the Avrami exponent will be less than 2. This is what is observed in the photoreaction of cinnamic acid reported here; our plots yield Avrami exponents of 1.6−1.7, indicative of one-dimensional growth with a decreasing nucleation rate.

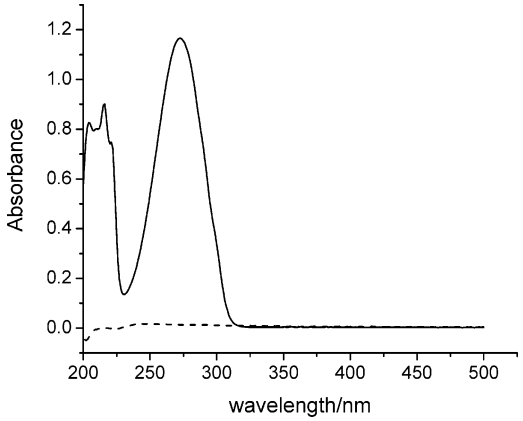

Figure 4. Solution-phase UV−vis spectra of cinnamic acid (solid line) and truxillic acid (dashed line). Both spectra have been corrected for solvent absorption.

Furthermore, Avrami exponents between 1 and 2 have been observed by Weinberg,[23] Wilkinson,[24] and Liu.[25] In those cases, the Avrami exponent was used to describe nucleation on the surface or at internal interfaces. As shown in Figure 4, cinnamic acid has a strong UV absorption, while truxillic acid has a comparatively weak absorption over the range of wavelengths studied here (280−400 nm). The microcrystalline powders used for this study are extremely optically dense, with a typical solid-state absorbance greater than 1.5 at wavelengths less than 325 nm (shown for a single-crystal sample of cinnamic acid, see Supporting Information). Powders of cinnamic acid crystals (100−500 μm) were prepared in a manner identical to single-crystal species used for the optical absorption measurements. This solid-state spectrum indicates that the light will be absorbed essentially quantitatively at the surface and not penetrate deep into the crystal to initiate reactions at internal interfaces. Furthermore, the growing layers of truxillic acid would not occlude the incoming radiation as the reaction progresses.

Overall, these data are consistent with the model that >90% of the light is absorbed on the cinnamic acid crystal surface. Thus, it is most likely that the photoreaction of α-*trans*-cinnamic acid is a nucleation and growth process that starts on the surface of the crystal when this range of wavelengths is used. The large dependence of the reaction rate on crystal shape and size that is observed in the literature[21] supports this theory because the surface area to volume ratio is heavily dependent on these two parameters.

The data also support the hypothesis of Enkelmann et al.[8] who postulated that α-*trans*-cinnamic acid forms α-truxillic acid heterogeneously when irradiated with broadband light. Experiments are currently underway in our laboratory to test the degree of homogeneity of this photoreaction at different wavelengths in the absorption band.

Conclusion

In conclusion, we have shown that solid-state photoreactions can be monitored effectively with solid-state NMR and that the

nucleation and growth model proposed by Johnson, Mehl, Avrami, and Kolmogorov is a potential framework for the reaction. The Avrami exponents obtained in our experiments on photoreactions of α-*trans*-cinnamic acid are indicative of a surface-initiated nucleation and growth process. Further experiments aim at the kinetics of the photodimerization process in cinnamic acid (and its derivatives) at various wavelengths along the absorption band. We hope to determine whether similar nucleation and growth mechanisms are manifested for different low-energy and high-energy photons.

Acknowledgment. The authors thank Professor Dewey Holten and Ms. H.L. Kee (Washington University) for assistance with the solid-state UV−vis absorption measurements and helpful discussions. Acknowledgment is made to the Donors of the American Chemical Society Petroleum Research Fund for partial support of this research and to the Alexander von Humboldt Foundation for providing a Lynen Postdoctoral Fellowship for M.B. We thank the National Science Foundation Summer Research Program in Solid-State Chemistry (DMR-0303450) for financial support of A.B.B.

Supporting Information Available: A solid-state UV−vis absorption spectrum in the range of 250−400 nm for a single-crystal sample of cinnamic acid. This material is available free of charge via the Internet at http://pubs.acs.org.

References and Notes

(1) MacGillivray, L. R.; Reid, J. L.; Ripmeester, J. A. *J. Am. Chem. Soc.* **2000**, *122*, 7817−7818.
(2) Cohen, M. D.; Schmidt, G. M. J. *J. Chem. Soc.* **1964**, 1996−2000.
(3) Feringa, B. L.; van Delden, R. A.; Koumura, N.; Geertsema, E. M. *Chem. Rev.* **2000**, *100*, 1789−1816.
(4) Feringa, B. L.; Jager, W.; de Lange, B. *Tetrahedron* **1993**, *37*, 8267−8310.
(5) Yokoyama, Y. *Chem. Rev.* **2000**, *100*, 1717−1739.
(6) Irie, M. *Pure Appl. Chem.* **1996**, *7*, 1367−1371.
(7) Berkovic, G.; Krongauz, V.; Weiss, V. *Chem. Rev.* **2000**, *100*, 1741−1753.
(8) Enkelmann, V.; Wegner, G.; Novak, K.; Wagener, K. B. *J. Am. Chem. Soc.* **1993**, *115*, 10390−10391.
(9) Kaupp, G. *Angew. Chem., Int. Ed. Engl.* **1992**, *31*, 592−595. (b) Kaupp, G. *Angew. Chem.* **1992**, *104*, 606−609.
(10) Allen, S. D. M.; Almond, M. J.; Bruneel, J. L.; Gilbert, A.; Hollins, P.; Mascetti, J. *Spectrochim. Acta, Part A* **2000**, *56*, 2423−2430.
(11) Ohba, S.; Ito, Y. *Acta Crystallogr., Sect. B* **2003**, *59*, 149−155.
(12) Harris, K. D. M.; Thomas, J. M. *J. Solid State Chem.* **1991**, *94*, 197−205.
(13) Zhang, J. H.; Krawietz, T. R.; Skloss, T. W.; Haw, J. F. *Chem. Commun.* **1997**, 685−686.
(14) Hwang, S. J.; Petucci, C.; Raftery, D. *J. Am. Chem. Soc.* **1998**, *120*, 4388−4397.
(15) Wright, J. D. *Molecular Crystals*; 1st ed.; Cambridge University Press: Cambridge, U. K., 1987; pp 112−113.
(16) Schaefer, J.; Stejskal, E. O. *J. Am. Chem. Soc.* **1976**, *98*, 1031−32.
(17) Opella, S. J.; Frey, M. H. *J. Am. Chem. Soc.* **1979**, *101*, 5854−5856.
(18) Steinfeld, J. I.; Francisco, J. S.; Hase, W. L. *Chemical Kinetics and Dynamics*, 2nd ed.; Prentice Hall: Upper Saddle River, NJ, 1999; pp 6−9.
(19) Johnson, W. A.; Mehl, R. F. *Am. Inst. Mining Metall. Eng., Inst. Met. Div., Tech. Publ.* **1939**, *1089*, 1−27.
(20) Avrami, M. *J. Chem. Phys.* **1939**, *7*, 1103−1112.
(21) Kolmogorov, A. N. *Bull. Acad. Sci. USSR, Phys. Ser.* **1937**, *1*, 355−359.
(22) Christian, J. W. *The Theory of Transformations in Metals and Alloys*; Pergamon: Oxford, U. K., 1981; pp 525−548.
(23) Weinberg, M. *J. Non-Cryst. Solids* **1991**, *134*, 116−122.
(24) Wilkinson, A.; Speck, J.; Cheetham, A. *Chem. Mater.* **1994**, *6*, 750−754.
(25) Liu, H.; Sullivan, R.; Hanson, J.; Gray, C.; Martin, J. *J. Am. Chem. Soc.* **2001**, *123*, 7564−7573.